Magneto-Optics: Direct and Inverse Effects

Thesis submitted under the supervision of
Dr. Muhammad Sabieh Anwar

by

Muhammad Waleed Khalid
Roll no. 2017-10-0124
Session 2013-2017

Department of Electrical Engineering,
Lahore University of Management Sciences, Lahore.

Acknowledgements

I would like to acknowledge the following people without whom I would not have been able to complete my work. My advisor, Dr. Muhammad Sabieh Anwar, for his undying support and motivation towards the project. He guided me all the way through till the end. He was always available and up to date with my work. He is a knowledgeable physicist, a modest person and someone I look up to as an ideal. Ali Akbar, PhD candidate at Department of Physics, LUMS. Ali has helped me in lab work and getting acquainted with optical instruments. I learned the use of optical instruments and setting up optical systems from his vast knowledge of experimental optics. Amrozia Shaheen, Senior Lab Instructor, for her help on Faraday Rotation setup, Stokes Polarimetry setup and interfacing of electromagnet's power supply with LabView. Khadim Hussain, junior lab technician, for connecting electromagnets to the chiller, cleaning of mount for the TGG crystal, filling of helium in cryostat compressor and changing its adsorber Hafiz Rizwan, senior lab technician, for crafting a mount for the TGG crystal, constructing a stand for holding instruments vertically, filling of helium in cryostat compressor and changing its adsorber. Ali Hassan, lab assistant, for helping with lab related issues and maintaining optics labs equipment. Arshad Maral, coordinator for Department of Physics, for assisting in all the logistical work.

Abstract

Magnetooptics deals with interaction between light and matter when matter is subjected to external magnetic field. Presence of external magnetic field varies optical anisotropy of the material. Different orientation of magnetic fields produces different magnetic effects. In the series of experiments performed at physics optics lab, magnetic circular and magnetic linear effects were observed in TGG crystal. Magnetic circular birefringence (MCB), Faraday effect, was observed at room temperature for 405 nm laser. Magnetic linear dichroism (MLD) and magnetic linear birefringence (MCB),Cotton-Mouton effect, was observed at cryogenic temperatures ranging from 8K-150K in TGG crystal. These two effects were observed for 405 nm and 633 nm laser. Complete stokes polarimetry using Fourier series coefficients was also done for observing magnetic linear effects,for 633 nm laser, in TGG crystal .

Contents

List of Figures

Chapter 1

Mathematical Representations of Light

1.1 Jones Calculus

A formula-ism used to describe the interaction of light and optical devices to predict the output of light. Studying the interaction of light with different devices can be used as en effective way to control polarization and can be used for technological purposes.

The polarization of light is described by column vectors, known as Jones vector

$$\begin{pmatrix} E_x \\ E_y \end{pmatrix} = e^{i\varphi} \begin{pmatrix} a \\ be^{i\delta} \end{pmatrix}$$

$e^{i\varphi}$ can be ignored since it the global phase and is common for both components of light. When light passes through an optical device, its polarization changes. Jones vectors should be normalized to avoid any inconsistencies in calculations. The effect of this optical device can me mathematically represented using a matrix, known as Jones matrix

$$\begin{pmatrix} E_x \\ E_y \end{pmatrix}_{in} = \begin{pmatrix} a_{11} & a_{12} \\ a_{21} & a_{22} \end{pmatrix} \begin{pmatrix} E_x \\ E_y \end{pmatrix}_{out}$$

Each of the optical element is represented by a matrix. By multiplying the matrices, a system matrix can be obtained. This system matrix describes the interaction between input light and the optical system. Jones calculus formation can only be used if we a have a completely polarized light and two

orthogonal components are coherent. An example of Jones calculus formation can be the following:

$$\begin{pmatrix} E_x \\ E_y \end{pmatrix}_{out} = \begin{pmatrix} 1 & 0 \\ 0 & 0 \end{pmatrix} \begin{pmatrix} e^{-i\phi_x} & 0 \\ 0 & e^{-i\phi_y} \end{pmatrix} \begin{pmatrix} \cos\theta & \sin\theta \\ -\sin\theta & \cos\theta \end{pmatrix} \begin{pmatrix} E_x \\ E_y \end{pmatrix}_{in}$$

matrices from left to right: *polarizer, retarder and rotator*

1.2 Stokes Parameters

Jones vectors can be used to described perfectly polarized light but in optical setups we do have to deal with partially polarized lights too so it would be valuable to have a set of vector which can handle this situation of partially polarized light too. Jones vectors describing two different waves cannot be added together except under the special circumstances where the beam are coherent with each other. So to describe the state of partially polarized Stokes parameters are used. These parameters can be formed together to make a Stokes vector. It should be noted that Stokes vector does not surpasses Jones vector, but rather compliments it. The representation used here is that of [**?**] (I,M,C and S).

Suppose there is an arbitrary wave that passes through a polarizer with transmission axis α. The intensity of wave is given by

$$I(\alpha) = {E_x}^2 \cos^2\alpha + {E_y}^2 \sin^2\alpha + E_x E_y \sin 2\alpha(\delta_x - \delta_y) \tag{1.1}$$

A simplified form of above expression is

$$I(\alpha) = A_0 + A_1 \cos 2\alpha + A_2 \sin 2\alpha \tag{1.2}$$

$$A_0 = \frac{1}{2}({E_x}^2 + {E_y}^2) \tag{1.3}$$

$$A_1 = \frac{1}{2}({E_x}^2 - {E_y}^2) \tag{1.4}$$

$$A_2 = E_x E_y \cos(\delta_y - \delta_x) \tag{1.5}$$

$${}_rA_2 = \mp E_x E_y \sin(\delta_y - \delta_x) \tag{1.6}$$

By making three measurements of intensity at different polarizer angles, amplitude, phase difference and orientation of the wave can be determined. It

will not have the information about the handedness of the rotation since cosine is an even function i.e. it will spit out same values for $(\delta_y - \delta_x) < 0$ and $(\delta_y - \delta_x) < 0$. After adding a QWP in the setup, an additional measurement using the same technique is made. This makes $(\delta_y - \delta_x)$ to $(\delta_y - \delta_x) \pm \frac{\pi}{2}$ where the sign of phase shift is on user's discretion and depends on the orientation of QWP. This has been labeled as ${}_rA_2$ in the description above. Now that all the ingredients for the Stokes parameters are present, these parameters can be defined.

$$I = Intensity$$

$$M = 2A_1 \tag{1.7}$$

$$C = 2A_2 \tag{1.8}$$

$$S = 2_rA_2 \tag{1.9}$$

A complete description of light requires complete information about all four Stokes parameters but three of them are independent and the fourth one can be determined using the relation

$$I^2 = M^2 + C^2 + S^2 \tag{1.10}$$

All these parameters are measured in the units of intensity. Please note that this equation cannot determine other parameters using this relation since it will be losing information regarding the sign of the parameter. Sign of these parameters are of intense importance. If M, C and S are known, I can be determined since it is an intensity and will always be positive.

1.3 Mueller Calculus

It is quite evident that as the wave passes through an optical element or system, its Stokes parameters will change. Now there is need of formalism that will describe this change in parameters. Stokes parameters in terms of a 4x1 column vector, known as the *Stokes Vector*. Each optical element is described by a 4x4 matrix, known as *Mueller Matrices*. All these matrices in the system are multiplied to get a system matrix. This system matrix multiplied by the input wave will give out the output Stokes vector. This

formalism is known as the *Mueller Calculus*.

$$\begin{pmatrix} I' \\ M' \\ C' \\ S' \end{pmatrix} = \begin{pmatrix} 1 & 0 & 0 & 0 \\ 1 & \cos 2\theta & \sin 2\theta & 0 \\ 0 & -\sin 2\theta & \cos 2\theta & 0 \\ 0 & 0 & 0 & 1 \end{pmatrix} \begin{pmatrix} I \\ M \\ C \\ S \end{pmatrix}$$

I, M, C and *S* are input Stokes parameters while *I', M', C'* and *S'* are output Stokes parameters. Input Stokes parameters change as they pass through the system described by a Mueller matrix.

Chapter 2

Magnetooptic Effects

2.1 Faraday Effect

When a material is subjected to magnetic field in the direction of parallel to propagation of direction of applied field, the plane of polarization is rotated. θ is the angle of rotation and is proportional to the magnitude of applied field, B,and the length of material along which the light passes through,d.

$$\theta = VBd \tag{2.1}$$

The constant V is called the Verdet constant and is defined as rotation per unit length per unit field strength. Verdet constant depends on the properties of medium, frequency of light, temperature T.

The anisotropy is explained by the different refractive indexes experienced buy the right circularly and left circularly polarized light after the application of magnetic field on the material. Due to difference in n_+ and n_-, the right circularly and left circularly polarized light travel at different velocities. The angle of rotation is given by

$$\theta = \frac{k_o}{2}(n_+ - n_-)d \tag{2.2}$$

2.1.1 Magnetic Circular Birefringence (MCB)

The difference in refractive index experienced by right and left circularly polarized light results in the rotation of plane of polarized light. The per-

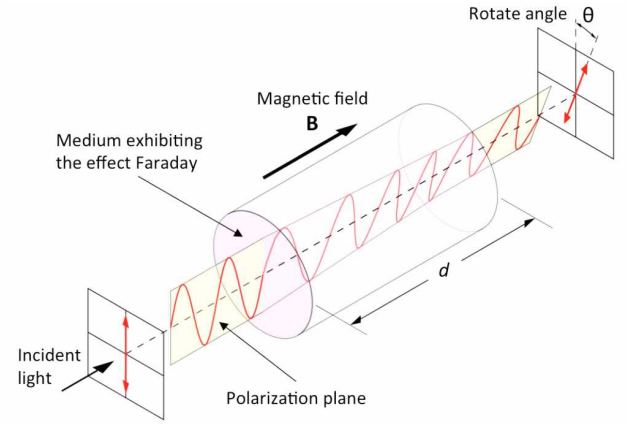

Figure 2.1: Faraday Effect in Crystals

mittivity tensor is given by [**?**]

$$\varepsilon = \begin{pmatrix} \varepsilon & -iQ & 0 \\ iQ & \varepsilon & 0 \\ 0 & 0 & \varepsilon \end{pmatrix} \tag{2.3}$$

where Q is directly proportional to magnetization, M, induced by the applied field B

Let z-axis be the direction of propagation of light so electric field can be defined as

$$E = E_{o_x} e^{i(\omega t - knz)} \hat{x} + E_{o_y} e^{i(\omega t - k_o nz)} \hat{y} \tag{2.4}$$

Eigen modes for a crystal under magnetic field applied in the direction of propagation of wave are right circular polarization,e_+ and left circular polarization e_-

$$e_+ = \frac{1}{\sqrt{2}} \begin{pmatrix} 1 \\ i \end{pmatrix} e^{i(\omega t - k_o n_+ z)} \tag{2.5}$$

$$e_- = \frac{1}{\sqrt{2}} \begin{pmatrix} 1 \\ i \end{pmatrix} e^{i(\omega t - k_o n_- z)} \tag{2.6}$$

$$\Delta n = n_+ - n_- \tag{2.7}$$

then the rotation angle θ is given by the following equation

$$\tan 2\theta = \tan(2k_o \Delta n z) \tag{2.8}$$

and the transfer matrix is given by [**?**]

$$T_F = \begin{pmatrix} \cos(k_o \Delta n z) & \sin(k_o \Delta n z) \\ \sin(k_o \Delta n z) & \cos(k_o \Delta n z) \end{pmatrix} \tag{2.9}$$

2.1.2 Magnetic Circular Dichroism (MCD)

If a medium exhibits different absorptions for right circularly and left circularly polarizations. A medium exhibiting MCD will change linear polarization to elliptical. Magnetic circular dichroism and magnetic circular birefringence are odd functions of magnetic field, B.

2.2 Cotton-Mouton Effect

Magnetic field applied transverse to the direction of propagation of wave results in the Cotton-Mouton effect. This effect is even in the magnetic field and depends on B^2 and results in change in ellipticity of circularly polarized light propagating through the medium.

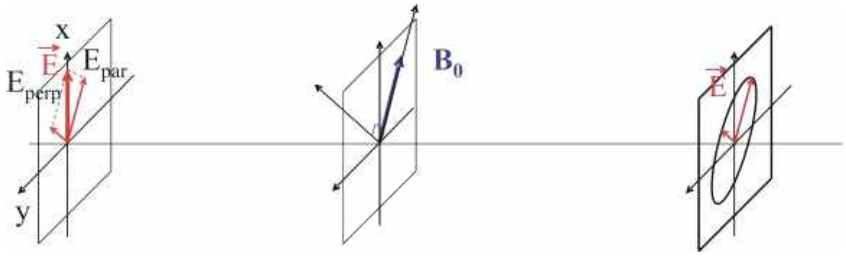

Figure 2.2: Cotton-Mouton effect

Crystals

Refractive n is related to permittivity by

$$n = \varepsilon_o \varepsilon_r \tag{2.10}$$

Isotropic crystal: all three axis offer same refractive index

$$\varepsilon_r = \begin{pmatrix} \varepsilon & 0 & 0 \\ 0 & \varepsilon & 0 \\ 0 & 0 & \varepsilon \end{pmatrix} \tag{2.11}$$

Uni-axial crystal: two axis offer same refractive index and axis offers different refractive index

$$\varepsilon_r = \begin{pmatrix} \varepsilon_{od} & 0 & 0 \\ 0 & \varepsilon_{od} & 0 \\ 0 & 0 & \varepsilon_{ex} \end{pmatrix} \tag{2.12}$$

Bi-axial crystal: all three axis offer different refractive indexes

$$\varepsilon_r = \begin{pmatrix} \varepsilon_{xx} & 0 & 0 \\ 0 & \varepsilon_{yy} & 0 \\ 0 & 0 & \varepsilon_{zz} \end{pmatrix} \tag{2.13}$$

2.2.1 Magnetic Linear Birefringence (MLB)

This effect is due to difference in the refractive experienced by the two orthogonal polarizations passing through a crystal. The crystal is placed in an applied magnetic field perpendicular to the direction of travel of wave. Linear polarization that has its angle oriented at an angle with the applied magnetic field, becomes elliptically polarize after passing through the medium.

The two normal modes for such orientation are

$$d_{\parallel} = \begin{pmatrix} 0 \\ 1 \end{pmatrix} e^{i(\omega t - k_o n_{\parallel} z)} \tag{2.14}$$

$$d_{\perp} = \begin{pmatrix} 1 \\ 0 \end{pmatrix} e^{i(\omega t - k_o n_{\perp} z)} \tag{2.15}$$

Linear birefringence, Δn, is responsible for the Cotton-Mouton Effect. where Δn

$$\Delta n = \left| n_{\parallel} - n_{\perp} \right| \tag{2.16}$$

Δn falls to zero when B goes to zero. The effect is revealed as the relative phase difference induced between the orthogonal components of polarizations as they travel through the crystal of length d

$$\delta = k_o \mathrm{Re}(n_\parallel - n_\perp)d \tag{2.17}$$

Linear birefringence is, Δn, is given by

$$(n_\parallel - n_\perp) = C_m \lambda B^2 \tag{2.18}$$

while the phase difference δ is given by

$$\delta = 2\pi C_m B^2 d \tag{2.19}$$

where C_m is the Cotton-Mouton constant of the material. The transfer matrix for a material of length d is given by [**?**]

$$T_{C_m} = \begin{pmatrix} e^{ik_o n_\parallel d} & 0 \\ 0 & e^{ik_o n_\perp d} \end{pmatrix} \tag{2.20}$$

2.2.2 Magnetic Linear Dichroism (MLD)

The difference in absorption coefficients of two orthogonal polarization is known as Magnetic Linear Dichroism. MLD results in rotation in the plane if polarization too as it passes through the medium. It is defined as

$$\Delta\alpha = \alpha_\parallel - \alpha_\perp = \mathrm{Im}(n_\parallel - n_\perp) \tag{2.21}$$

2.2.3 Combining Magnetic Linear and Circular Birefringence

Combining the effects of MLB and MCB can be used in various applications. When an isotropic crystal is exposed magnetic fields in both axial and transverse orientations, permittivity tensor takes the following form [**?**]

$$\varepsilon(B) = \begin{pmatrix} \varepsilon_{11}(B^2) & -iQ(B) & 0 \\ iQ(B) & \varepsilon_{12}(B^2) & 0 \\ 0 & 0 & \varepsilon_{33}(B^2) \end{pmatrix} \tag{2.22}$$

The diagonal terms re responsible for MLB and off diagonal terms are responsible for MCB. Complex parts of diagonal terms are responsible for MLD and complex parts in off diagonal terms are responsible for MCD.

2.3 Magnetooptical Kerr Effect (MOKE)

With a lot of magnetooptical effects that take place as light passes through a magnetized material, a number of effects can be observed as light is reflected from magnetized surface. These are known are Kerr effects and there are three types if Kerr effects. These effects are linear with B.

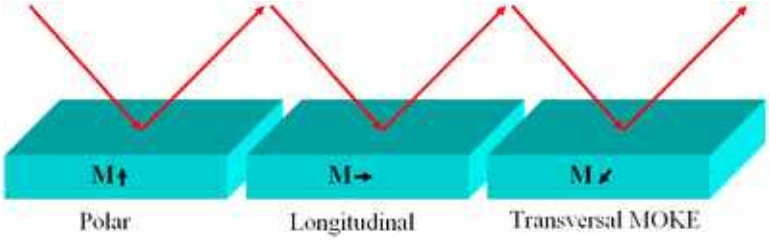

Figure 2.3: Geometries of MOKE

2.3.1 Polar Kerr Effect

There is rotation in the plane of polarization and generation of ellipticity when linearly polarized light is reflected from the surface that is magnetized normally to the surface.

2.3.2 Longitudinal Kerr Effect

Rotation in the plane of polarization and ellipticity is observed when a linearly polarized light. In this geometry, magnetization vector lies in plane of incidence of light and sample plane. This geometry is used in the observation of domain structure of a material whose magnetization lies in the sample plane

2.3.3 Transverse Kerr Effect

It is observed only for absorbing materials. It manifests itself as variation in intensity and phase of linearly polarized light reflected from magnetized material,. The magnetization lies in the plane of sample but perpendicular to plane of incidence of light.

Chapter 3

Measurement of Magnetic Circular Birefringence (Faraday Effect) using Phase Sensitive Detection

3.1 Experiment

Faraday effect is measured in TGG crystals placed in oscillatory fields of frequency Ω,

$$B = B_o \cos(\Omega t) \tag{3.1}$$

Since the field is oscillatory the rotation angle is oscillatory and a function of Ω,

$$\theta = \theta_o \cos(\Omega t) \tag{3.2}$$

3.1.1 Setup

Laser (405 nm) passes through a polarizer set at 0^o. This polarizer sets up the coordinate system. Laser then passes through the magnetized TGG crystal, where the direction of oscillatory applied magnetic field is in direction of propagation of laser. TGG is a uniaxial crystal in the absence of external magnetic field and it changes its behavior when it is subjected to an external magnetic field. In this experiment, an oscillatory magnetic field is produced by Helmholtz coil. Current from signal generator is fed to an amplifier and

this amplifier provides current to Helmholtz coil. To obtain minimum resistance, frequency of this AC signal is the resonant frequency of Helmholtz coils. Another polarizer (analyzer)is placed for detection of light emerging from the crystal before laser finally falls on to the photodetector. Photodetector converts light intensity into current. Current from the photodetector is then fed to lock-in amplifier. Reference signal required by the the lock-in amplifier is AC signal given to the Helmholtz coil. Lock-in extracts the AC signal from output it receives from the photodetector.

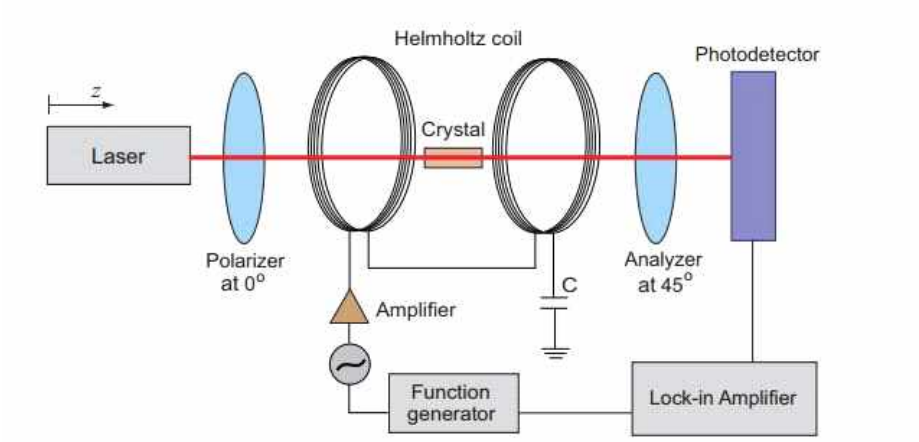

Figure 3.1: Faraday Rotation Schematic

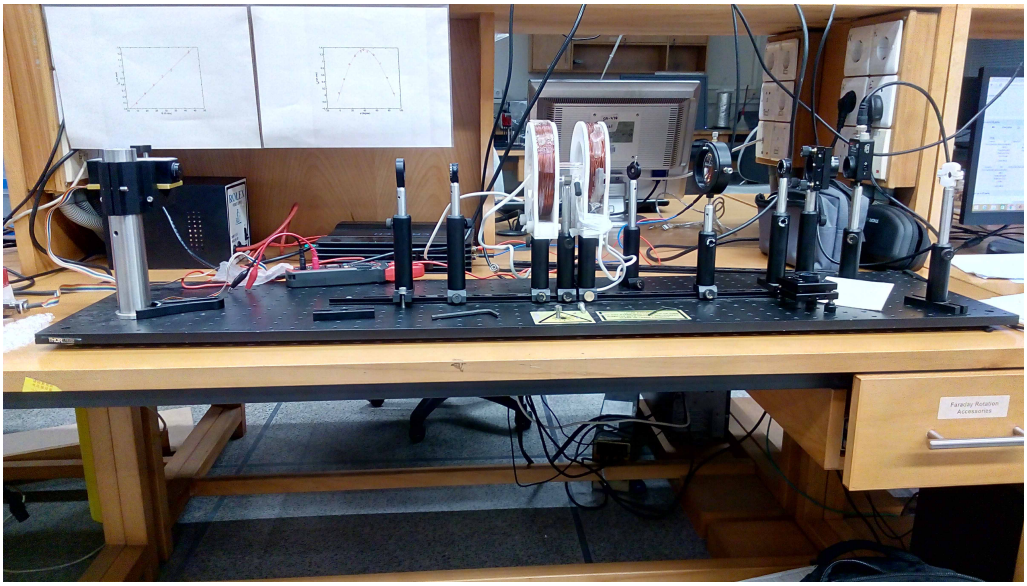

Figure 3.2: Lab setup

3.1.2 Mathematical Analysis

Jones calculus representation of this system is given by

$$\begin{pmatrix} \cos^2\phi & \sin\phi\cos\phi \\ \sin^2\phi & \sin\phi\cos\phi \end{pmatrix} \begin{pmatrix} \cos\theta & -\sin\theta \\ \sin\theta & \cos\theta \end{pmatrix} \begin{pmatrix} 1 & 0 \\ 0 & 0 \end{pmatrix}$$

When a unpolarized light is incident on this system, the intensity of output light (normalized) is given by

$$I = \cos^2(\phi - \theta) \tag{3.3}$$

To maximize the sensitivity of the detection system, analyzer angle ϕ is optimized by maximizing $\frac{dI}{d\phi}$

$$\frac{dI}{d\phi} = \sin(2(\phi - \theta)) \tag{3.4}$$

$$\frac{d^2I}{d\phi^2} = \cos(2(\phi - \theta)) \tag{3.5}$$

since $\theta << \phi$, $\frac{dI}{d\phi}$ is maximum for $\phi = 45^o$ [**?**]

3.2 Determination of Verdet constant

Since photodetector converts intensities into current, current has an ac component, i_{ac}, and a dc component i_{dc}. Total current is given by

$$i = i_{ac} + i_{dc} \tag{3.6}$$

Rotation angleθ is related to current by

$$\theta_o = \frac{i_{ac}}{\sqrt{2} i_{dc}} \tag{3.7}$$

$$\theta_{rms} = \frac{\theta_o}{\sqrt{2}} \tag{3.8}$$

i_{dc} is measured by connecting photodetector's output to a voltmeter via an I/V converter of known resistance. For i_{ac}, magnetic field is increased, by increasing the input current to Helmholtz coil, and the output current from the Lock-in amplifier is noted down. Verdet constant can be determined using the first and second harmonics of of i_{ac} from the lock-in amplifier [**?**]. For first harmonic,

$$i_{ac} = 2 i_{dc} V B d \sin(2\phi) \tag{3.9}$$

for second harmonic,

$$i_{ac} = 2 i_{dc} (V B d)^2 \cos(2\phi) \tag{3.10}$$

3.3 Results

Results for output current versus magnetic field is plotted for first and second harmonics. Equations (3.9) and (3.10) are used to determine Verdet constant of TGG crystal. TGG crystal is of the length 1 cm and diameter 3 mm. Literature value of Verdet constant is 464 rad/Tm [**?**]

3.3.1 Determination using first harmonic

The analyzer angle is ($\phi = 45^o$) and V is given by

$$V = \frac{i_{ac}}{2 i_{dc} B d} \tag{3.11}$$

Verdet constant was found to be 453 ± 9 rad/Tm using the first harmonic.

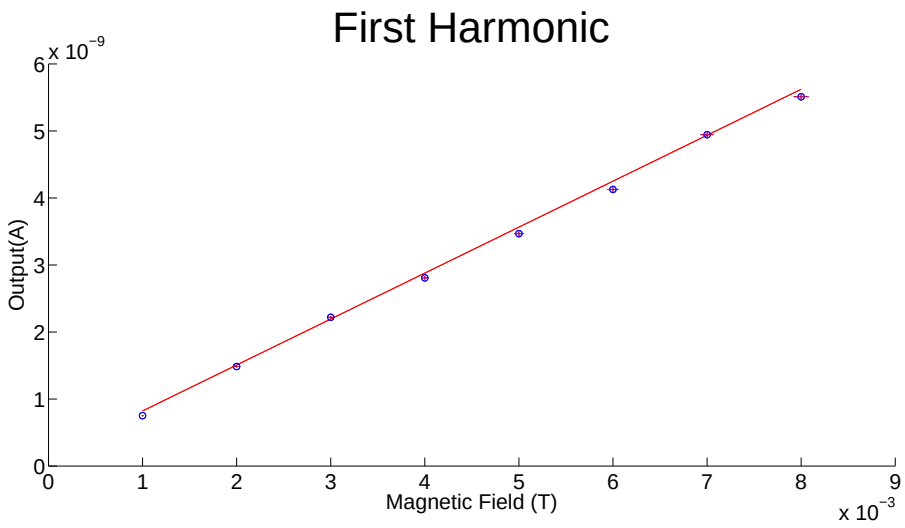

Figure 3.3: First harmonic v. magnetic field

3.3.2 Determination using second harmonic

The analyzer angle is ($\phi = 0^o$) and V is given by

$$V = \sqrt{\frac{i_{ac}}{2i_{dc}(Bd)^2}} \tag{3.12}$$

Verdet constant was found to be 333 ± 5 rad/Tm using the second harmonic. Since there was considerable amount of noise in second harmonic, the Verdet constant deviated more from the literature value.

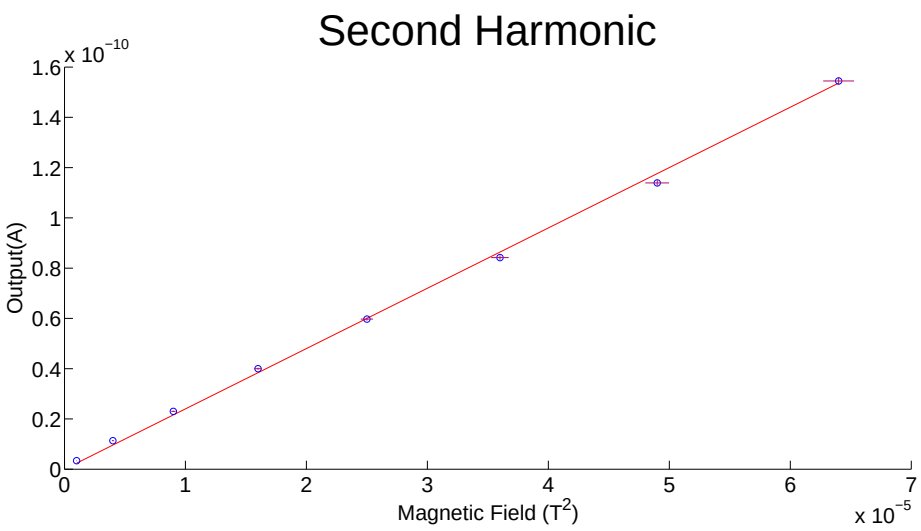

Figure 3.4: Second harmonic v. magnetic field

Chapter 4

Measurement of Magnetic Linear Effects

The Jones calculation formulation for the suggested experimental technique is given by

$$\begin{pmatrix} E_x \\ E_y \end{pmatrix} = \begin{pmatrix} \cos^2\alpha & \sin\alpha\cos\alpha \\ \sin\alpha\cos\alpha & \sin^2\alpha \end{pmatrix} \begin{pmatrix} e^{i\Delta\beta d/2} & 0 \\ 0 & e^{-i\Delta\beta d/2} \end{pmatrix} \frac{1}{\sqrt{2}} \begin{pmatrix} 1 \\ 1 \end{pmatrix}$$

where $\Delta\beta = k_o\Delta n$, α is the angle of the analyzer and d is the length of crystal through which light passes through.$\Delta\beta$ has a real part and an imaginary part.

$$\Delta\beta = \Delta\beta' + i\Delta\beta \tag{4.1}$$

The output intensity I of the light defined by

$$I = \left|E^\dagger E\right| \tag{4.2}$$

where $E^\dagger$ is the conjugate transpose of the output vector of light. The intensity in this case is given by

$$I = \frac{1}{2}(\cosh(\Delta\beta" d) + \sinh(\Delta\beta" d)\cos(2\alpha) + \cos(\Delta\beta' d)\sin(2\alpha)) \tag{4.3}$$

To extract out magnetic linear dichroism (MLD) from the intensity equation, α is kept at 0^o. Equation for MLD takes the form

$$\Delta n" = \frac{1}{k_o d}\ln(I) \tag{4.4}$$

To extract out magnetic linear birefringence (MLB) from the intensity equation, α is kept at 45^o. Equation for MLB takes the form

$$\Delta n = \frac{1}{k_o d} \arccos(2I - \cosh(\Delta\beta" d)) \tag{4.5}$$

Data for β" is used from the experiment performed for MLD

Rotation and Ellipticity

Rotation angle θ is given by

$$\tan(2\theta) = \frac{\cos'(\beta d)}{\sinh(\beta d)} \tag{4.6}$$

Ellipticity angle ψ is given by

$$\sin(2\psi) = \frac{\sin'(\beta d)}{\cosh(\beta d)} \tag{4.7}$$

Experiment Overview

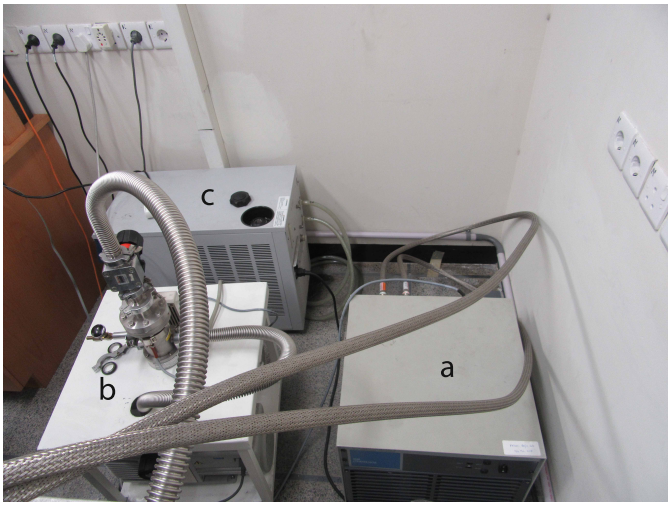

Figure 4.1: Cryostat (a) compressor (b) rotary and TMP (c) chiller

Experiment was performed at cryogenic temperatures ranging from 8k to 150K. Transverse DC magnetic field was applied to the uniaxial TGG crystal.

An input linear polarization at 45^o was incident to the crustal placed in the vicinity of the DC magnetic field. The light sources were 405 nm (BW Tek, BWI-405-40E) and 633 nm (Thorlabs,HNL100L) . The transmission axis of the linear polarizer P was fixed along the 45^o. The TGG crystal (Castech Inc.) is cylindrical in shape with a length of 1 cm and diameter of 3 mm. The laser beam is incident on the circular cross-section of the cylinder along the designated optical axis (z axis) of the uniaxial crystal. The crystal was mounted inside the vacuum shroud of the cryostat (Janis Research) using a devised clamping assembly made out of 99.9 percent pure copper. Thermal grease (Apiezon) was applied between the sample holder and the cold-head of the cryostat in order to maximize thermal conductivity. Fused quartz windows on the sides of the vacuum shroud allowed laser beam access to the crystal inside. A computer interfaced temperature controller (Model 331, LakeShore) was used to vary the temperature from 8150 K using a 25 W resistive heater while the temperature of crystal was monitored using a Gallium Arsenide diode temperature sensor (TG-120-CU-4L, LakeShore).

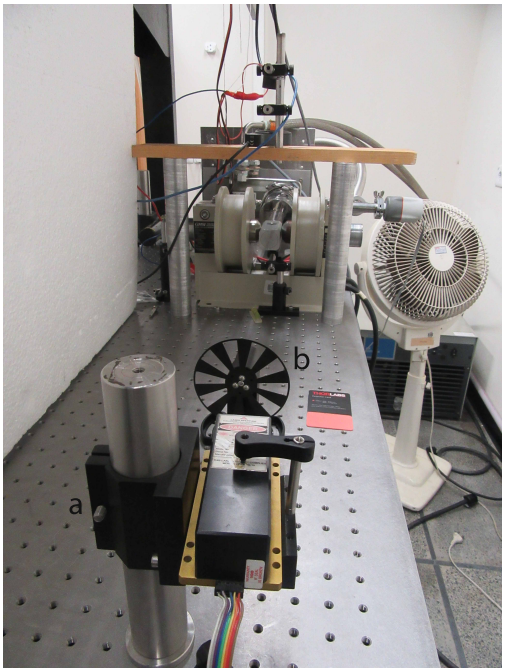

Figure 4.2: Front view (a) laser (b) optical chopper

An electromagnet (3470, GMW Associates) was used as the magnetic field source. The electromagnets power supply (DLM60-10, Sorensen) as well as the temperature monitoring and control system were fully integrated using LABView allowing automated scanning of the magnetic field and temperature for rapid measurements. The magnetic field B was controlled by varying the current passing through the electromagnet coils. The calibration constant relating current and magnetic field was pre-determined using a gauss meter (410-SCT, LakeShore).After passing through the crystal placed in cryostat, light passes through the analyzer and then to photodetector. Output from photodetector is fed to lock-in amplifier (SR830, Stanford Research Systems)allowing phase sensitive detection. Lock-in amplifier is connected to the computer to store the readings from the lock-in amplifier Optical chopper was used for modulation of light at 500 Hz and the reference signal for the lock-in amplifier is given from the optical chopper.

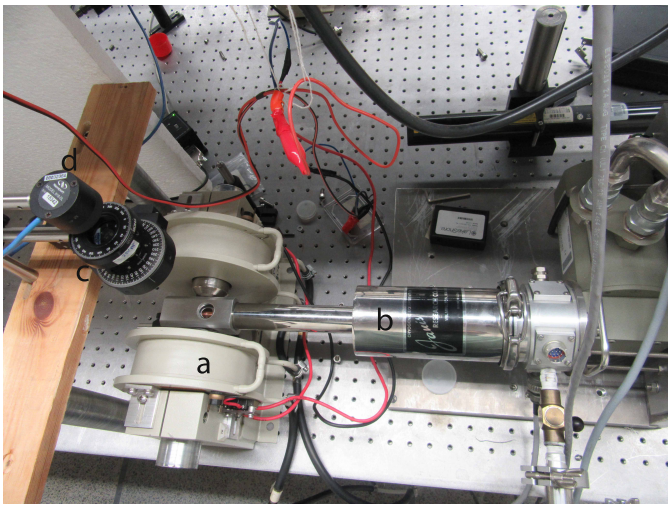

Figure 4.3: Top view (a) electromagnet (b) vacuum shroud (c) analyzer (d) detector

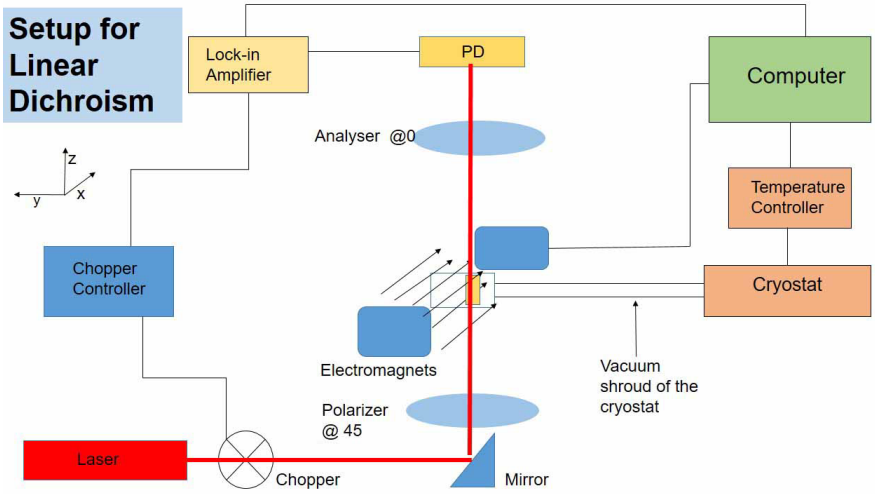

Figure 4.4: MLD setup

4.1 Measurement of Magnetic Linear Dichroism

4.1.1 Experimental Setup

4.1.2 Results

Equation 4.4 is used to extract out MLD from the output intensity. At $B = 0$, dichroism is 0 since the crystal is isotropic in the absence of any external magnetic field. As the magnitude B increases, magnetically induced dichroism also increases. Fig 4.4 and 4.7 shows temperature dependance of MLD. It shows an inverse relation between MLD and temperature. Since magnetization increases at low temperatures, magnetic effects also tend to increase. These results were later used for the calculation of MLB, rotation and ellipticity shown in next section.

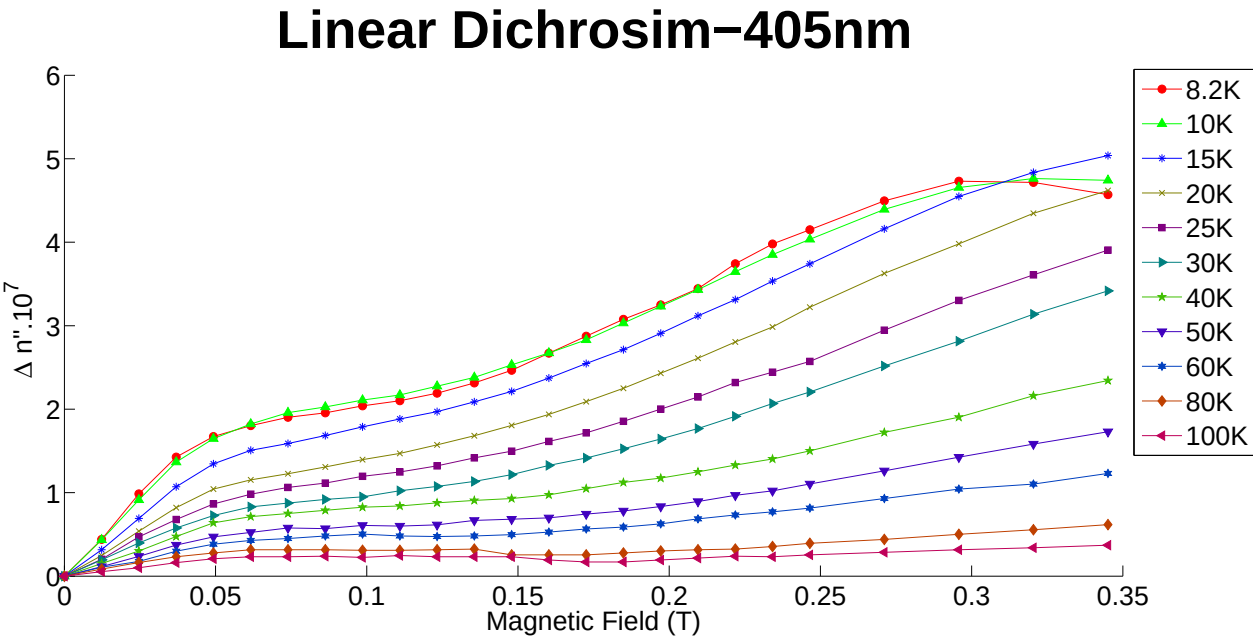

Figure 4.5: Variation of MLD with B at different temperatures 405 nm

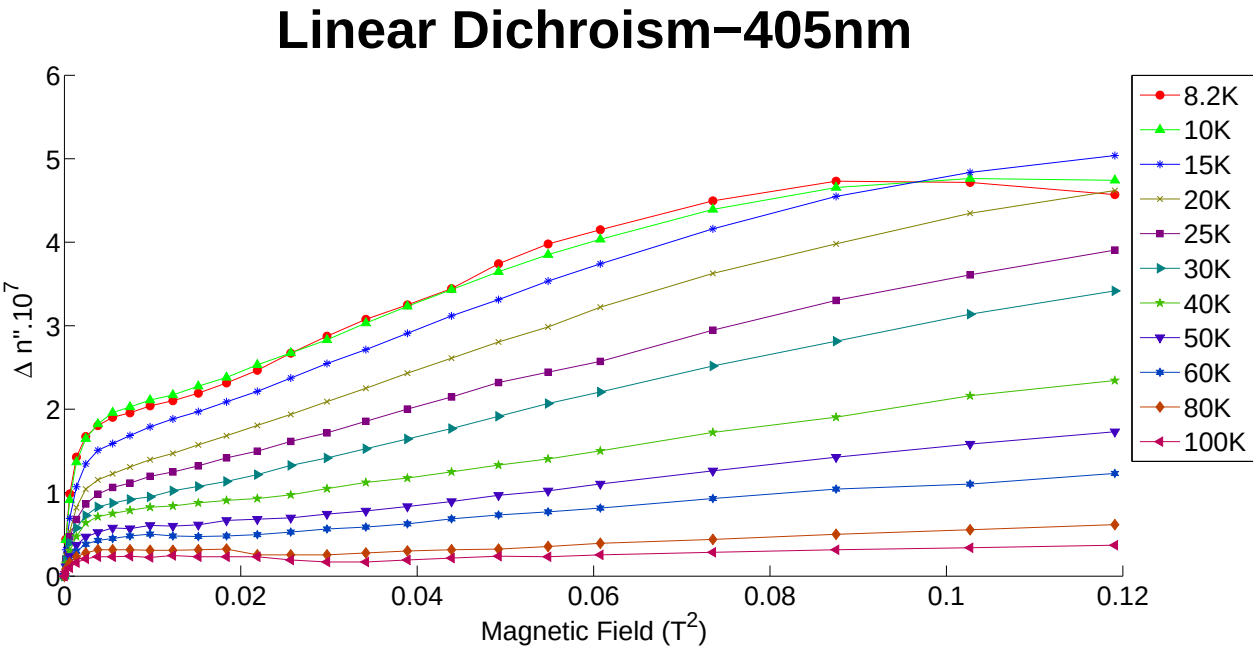

Figure 4.6: Variation of MLD with B^2 at different temperatures 405 nm

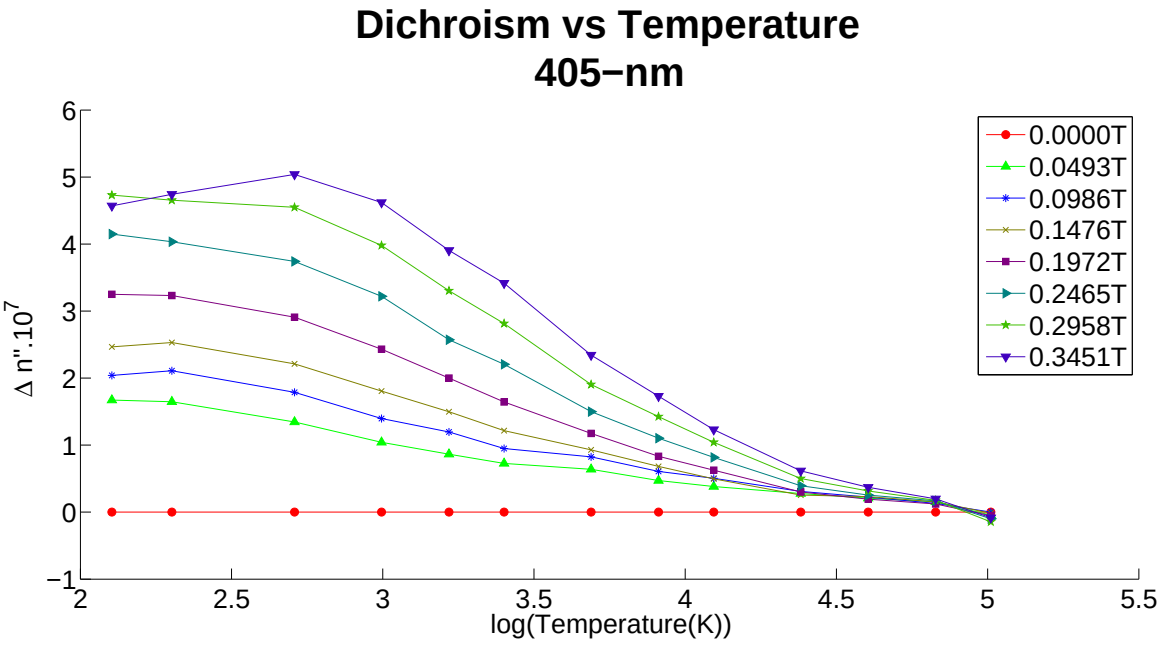

Figure 4.7: Variation of MLD with temperature at different B 405 nm

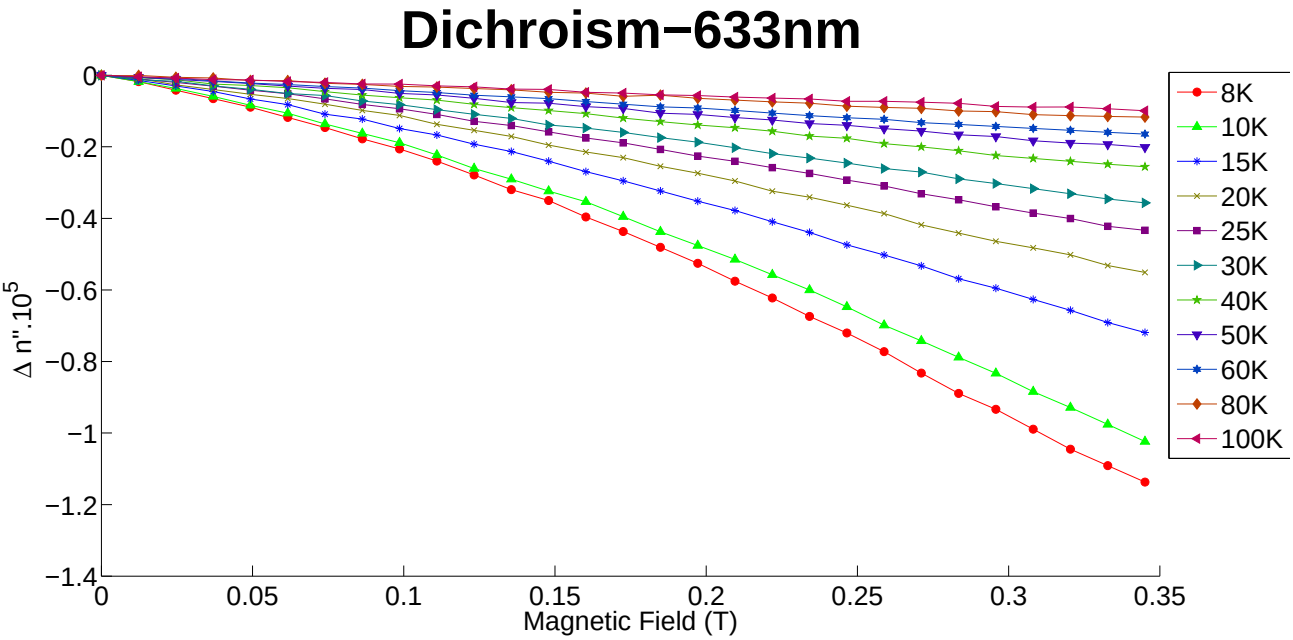

Figure 4.8: Variation of MLD with B at different temperatures 633 nm

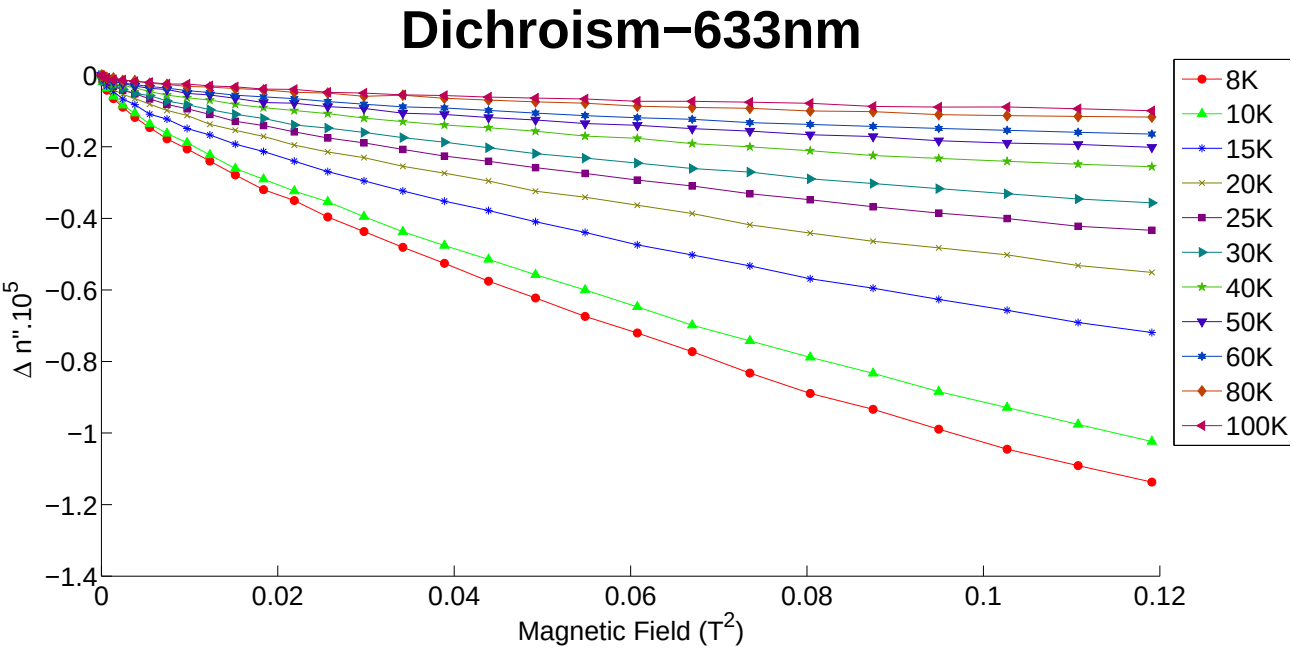

Figure 4.9: Variation of MLD with B^2 at different temperatures 633 nm

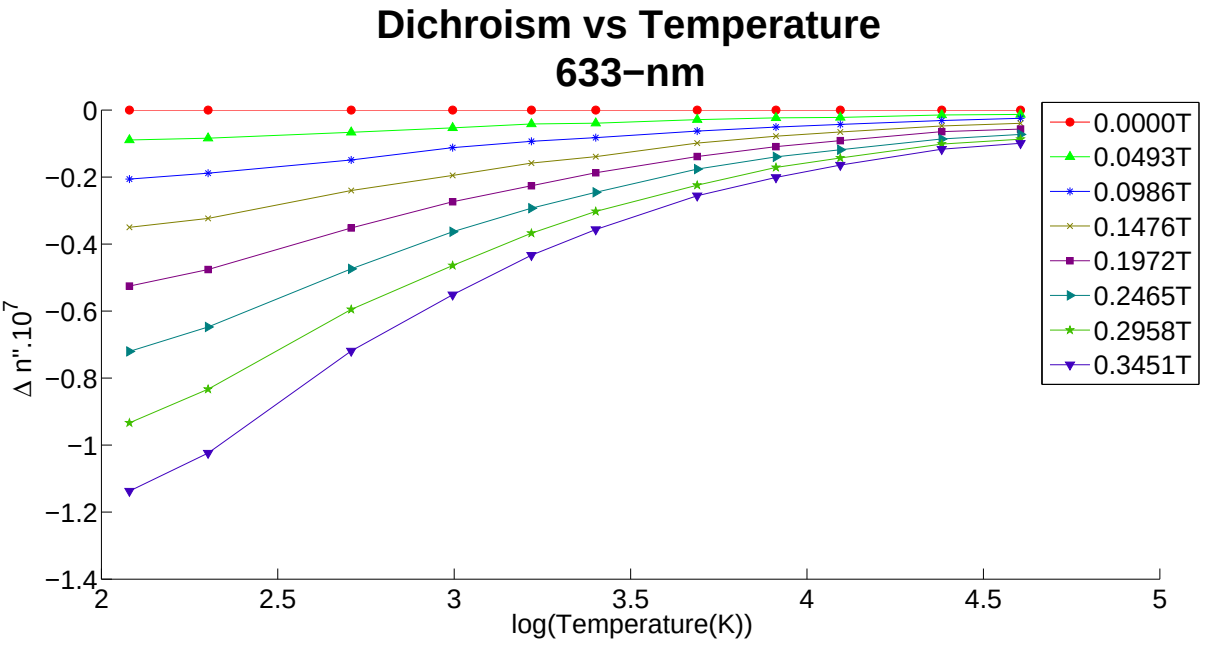

Figure 4.10: Variation of MLD with temperature at different B for 633 nm

4.2 Measurement of Magnetic Linear Birefringence (Cotton-Mouton Effect)

4.2.1 Experimental Setup

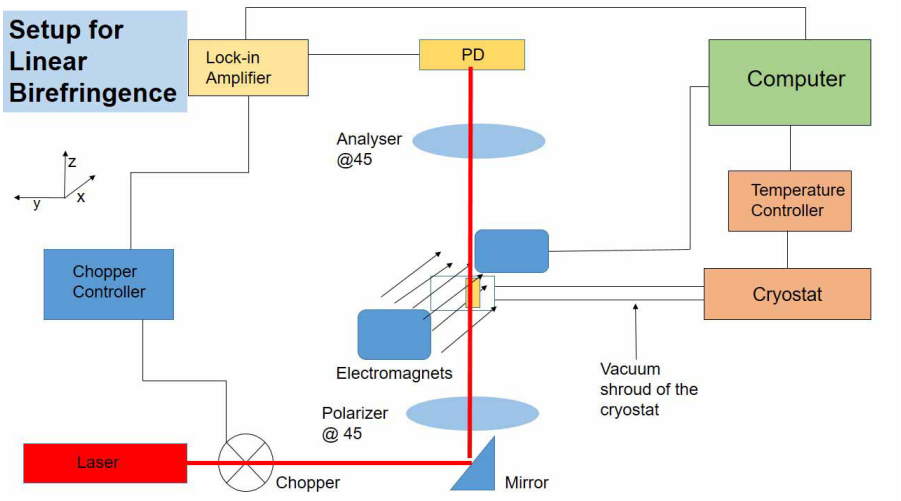

Figure 4.11: MLB setup

4.2.2 Results for MLB

Results for the experiment are shown below for 405 nm and 633 nm lasers

Equation 4.5 is used to extract MLB from the output intensity. At $B = 0$, birefringence is 0 since the crystal is isotropic in the absence of any external magnetic field. As the magnitude B increases, magnetically induced birefringence also increases. Fig 4.11 and 4.14 shows temperature dependance of MLB. It shows an inverse relation between MLB and temperature, same as that of MLD. Since magnetization increases at low temperatures, magnetic effects also tend to increase. In the next section, these results are used in calculation of rotation and ellipticity of the emerging beam which describes the change in polarization ellipse as light passes through the magnetized crystal.

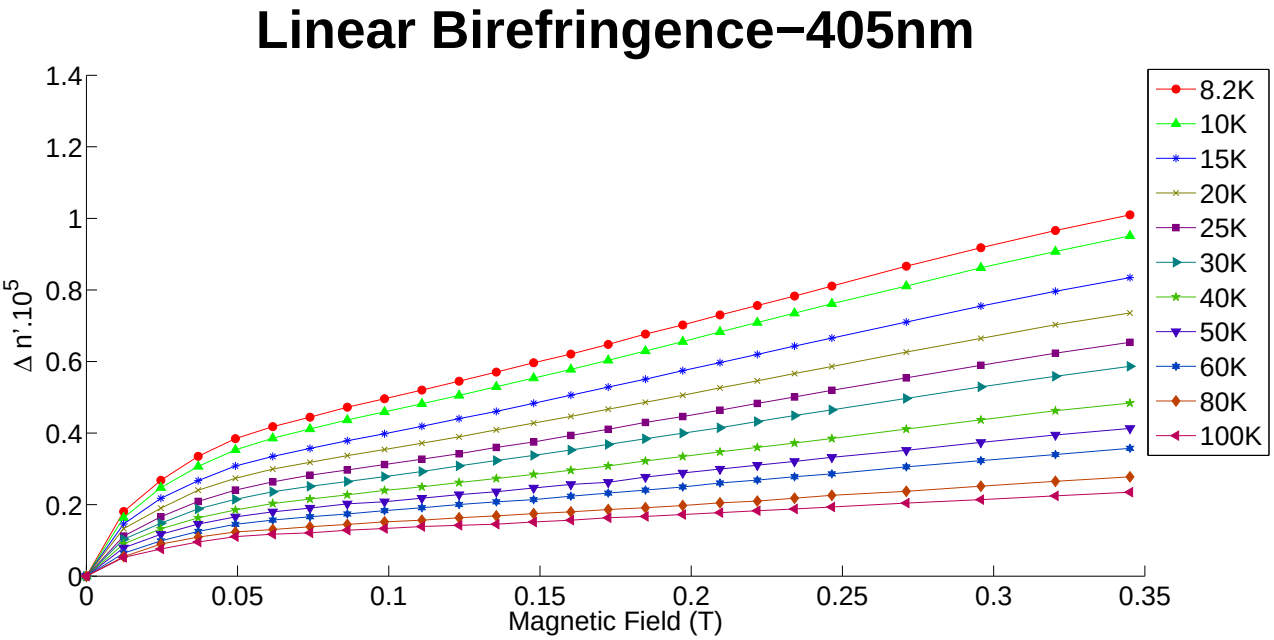

Figure 4.12: Variation of MLB with B at different temperatures 405 nm

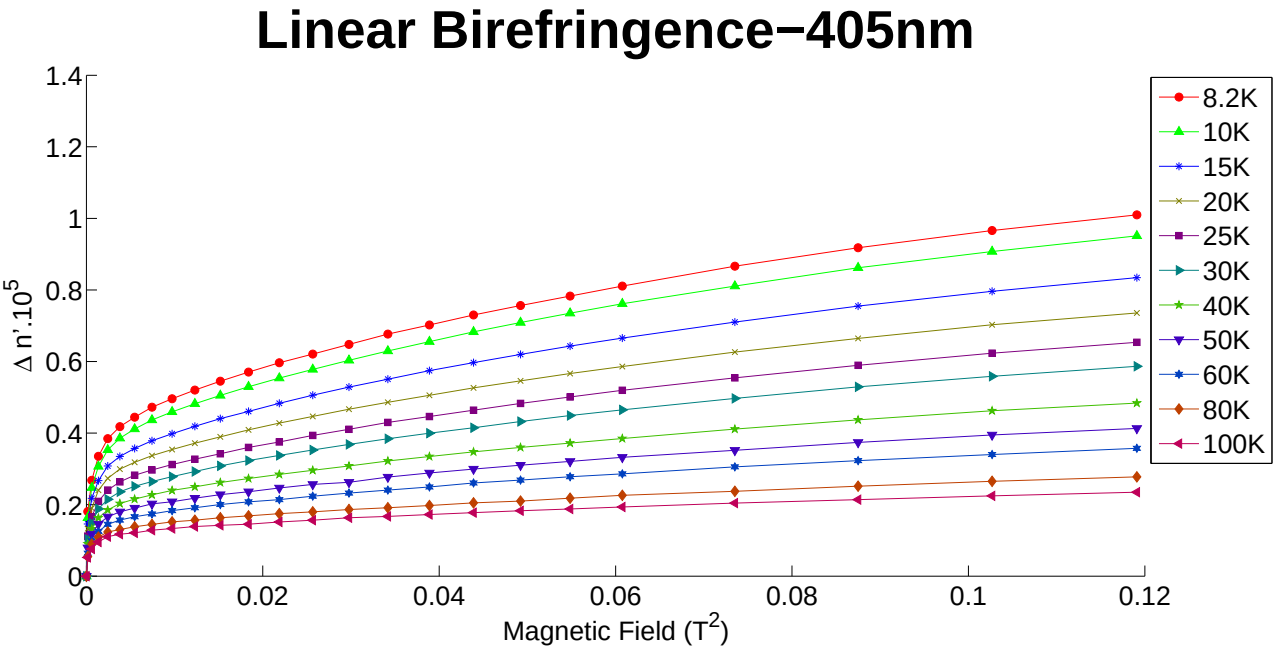

Figure 4.13: Variation of MLB with B^2 at different temperatures 405 nm

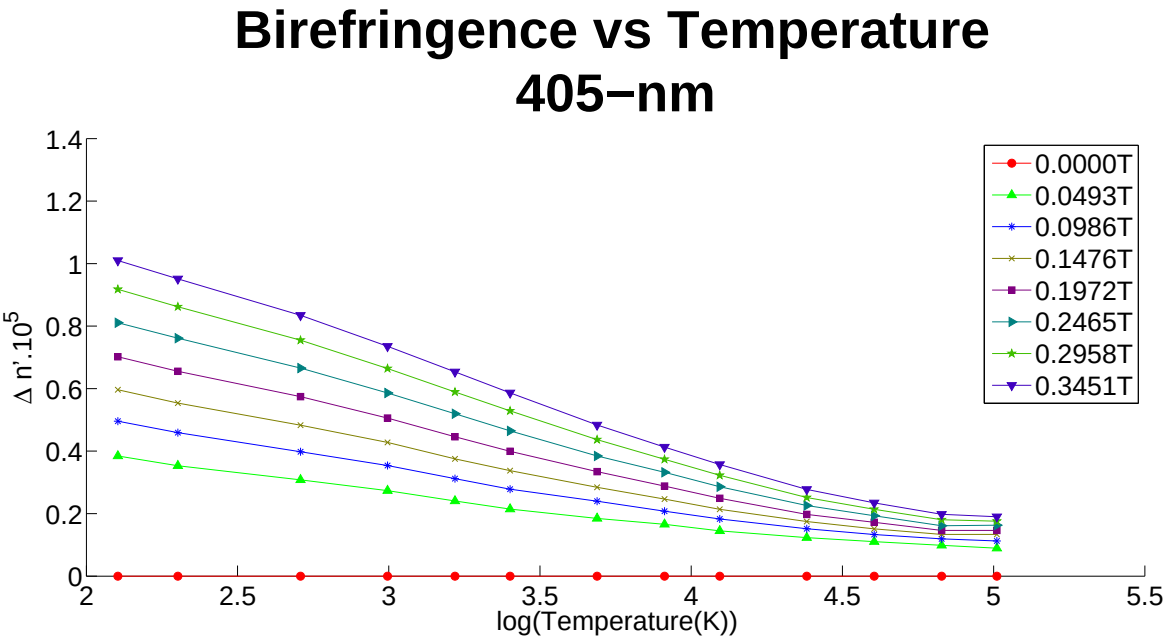

Figure 4.14: Variation of MLB with temperature at different B for 405 nm

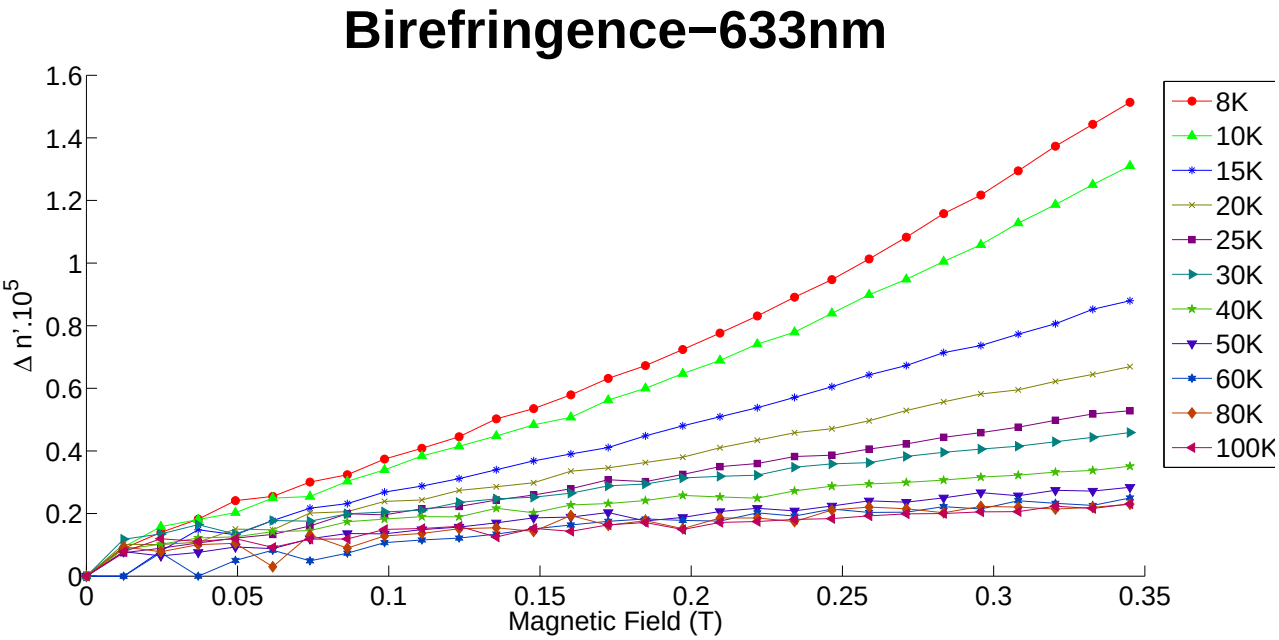

Figure 4.15: Variation of MLB with B at different temperatures 633 nm

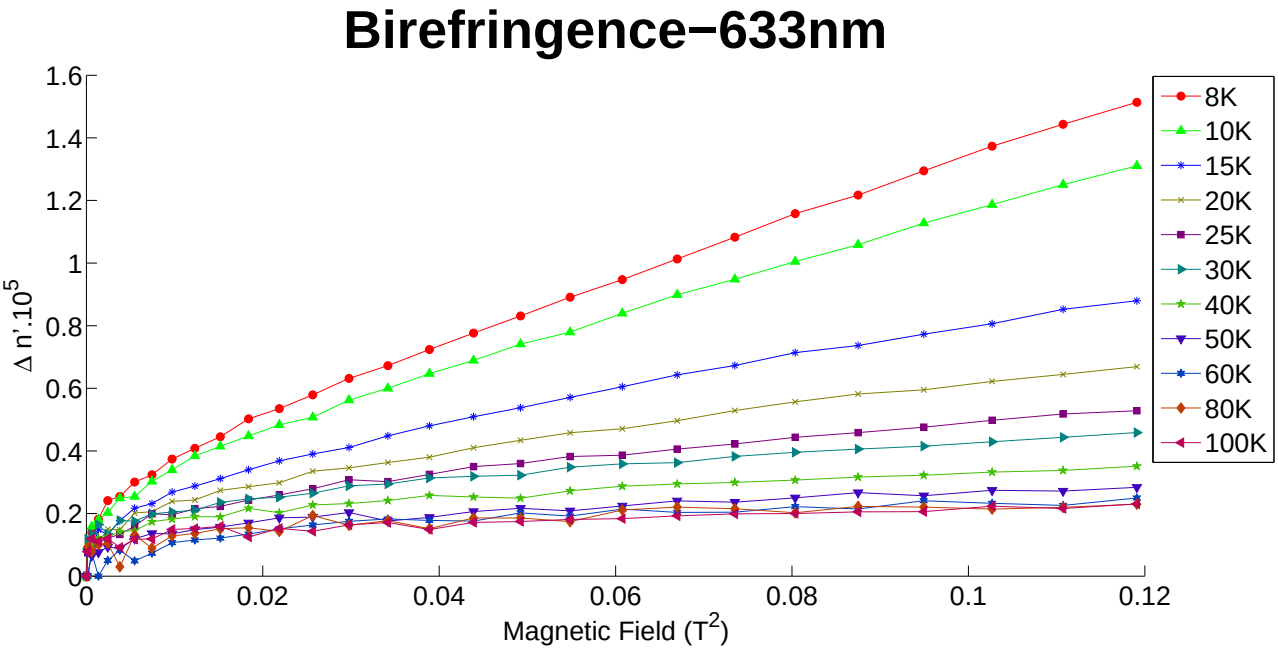

Figure 4.16: Variation of MLB with B^2 at different temperatures 633 nm

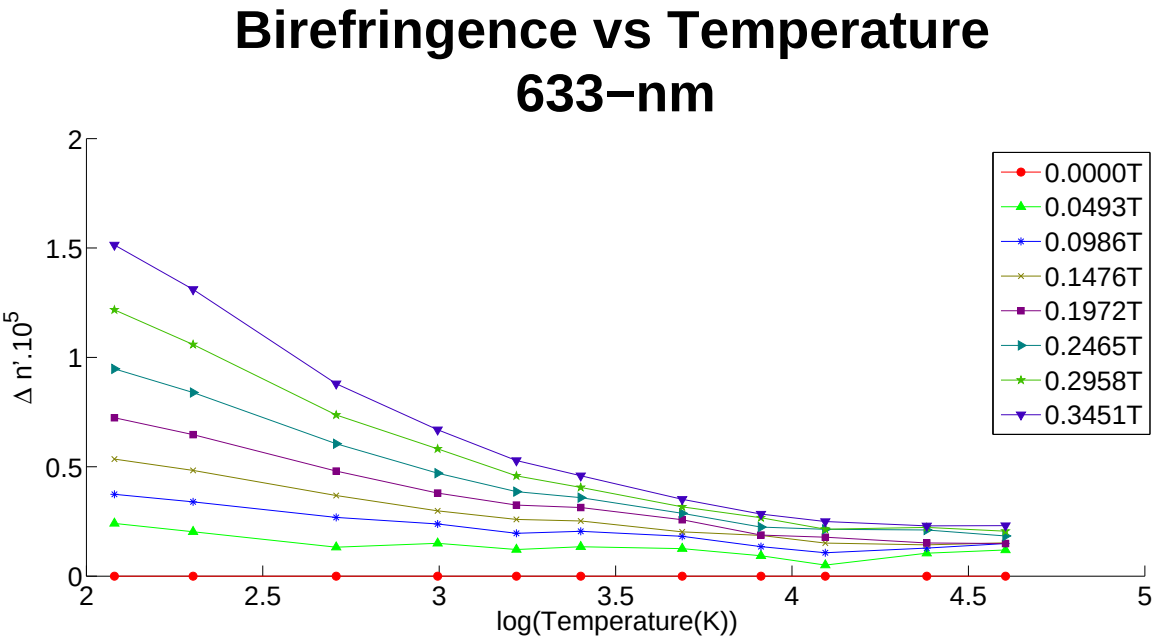

Figure 4.17: Variation of MLB with temperature at different B for 633 nm

4.3 Rotation and Ellipticity

Equations 4.6 and 4.7 are used to calculate rotation and ellipticity of the emergent beam. As discussed in section 2.2, MLD causes rotation in plane of polarization of light and MLB causes phase shift between two normal modes (horizontal and vertical polarizations) passing through a magnetized crystal. Ellipticity and rotation tend to increase with increase in B since MLB and MLD are increasing. Results are shown below

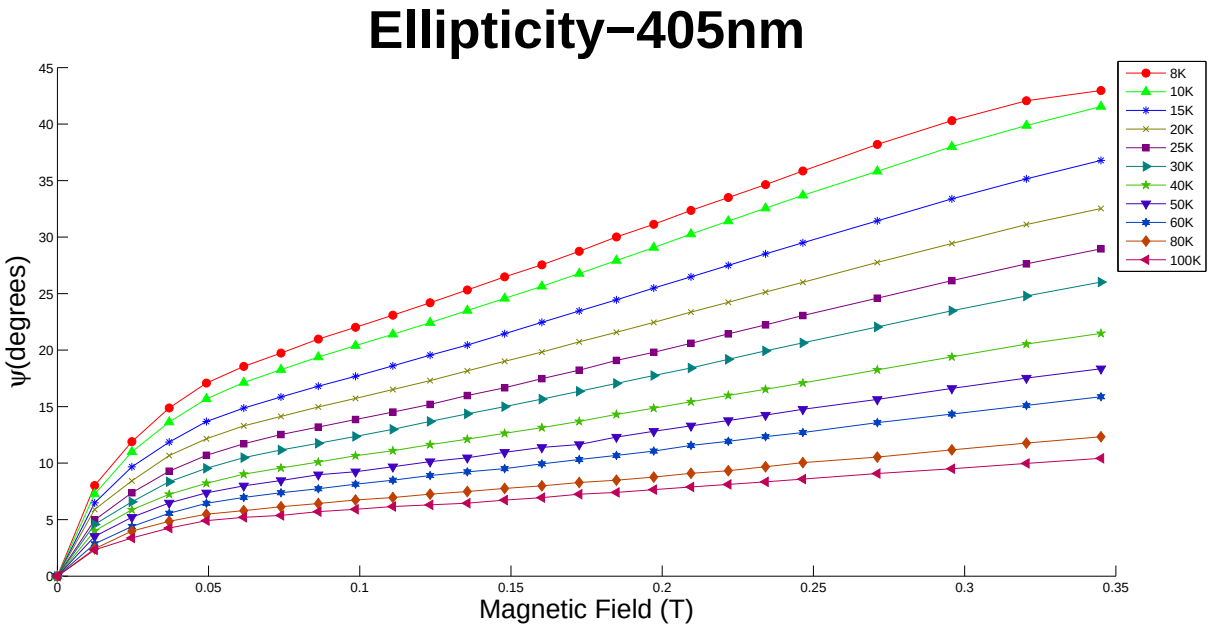

Figure 4.18: Ellipticity v B for 405 nm

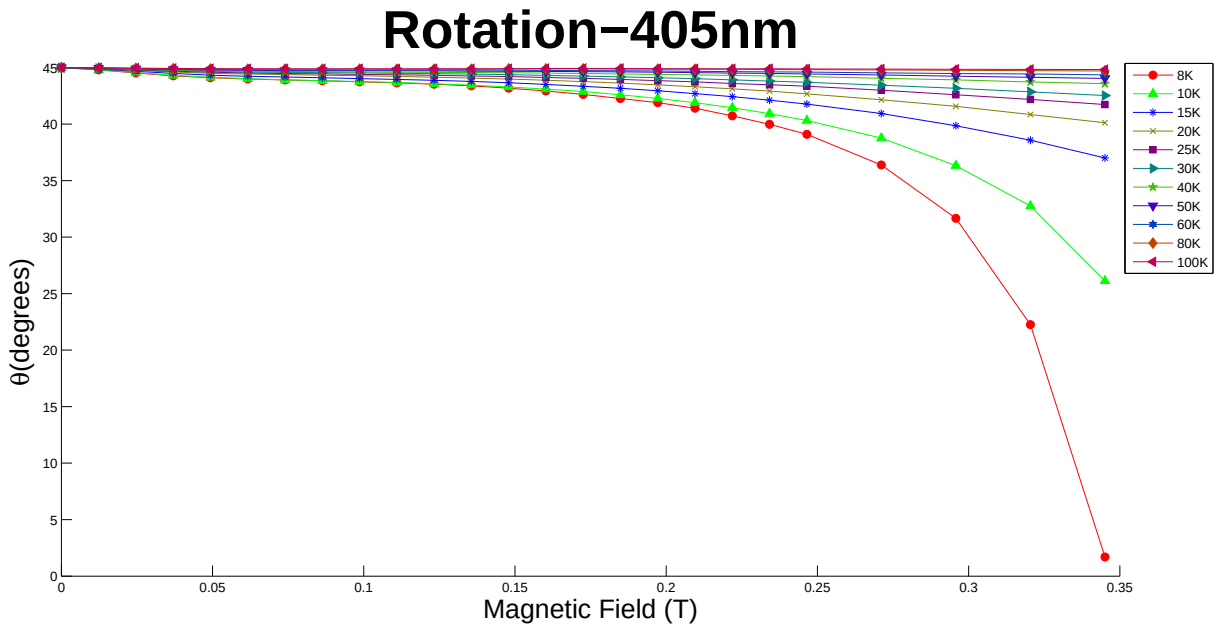

Figure 4.19: Rotation v B for 405 nm

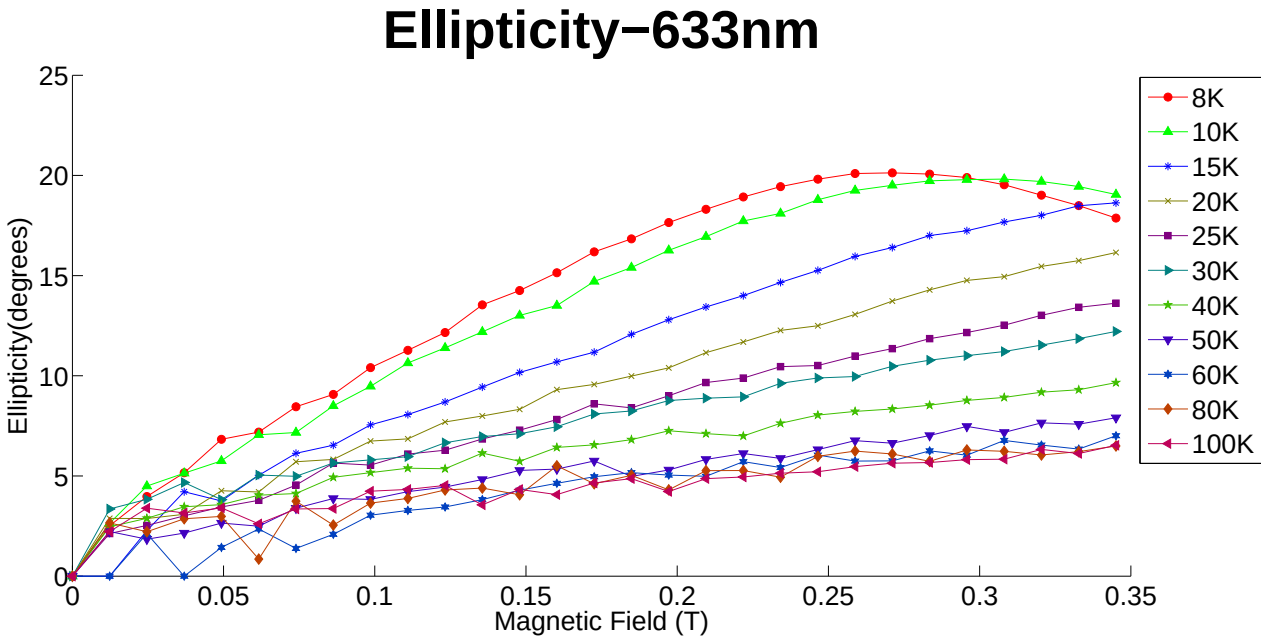

Figure 4.20: Ellipticity v B for 633 nm

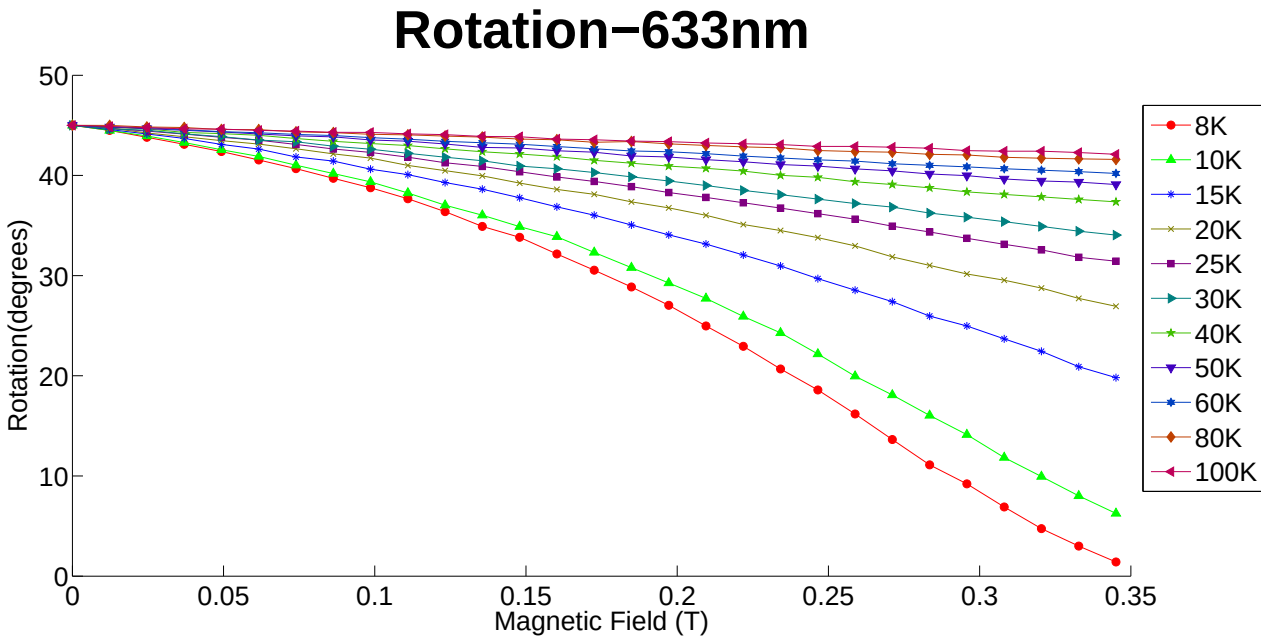

Figure 4.21: Rotation v B for 633 nm

Chapter 5

Stokes Polarimetry Using Fourier Series Coefficients

The Stokes parameters of any polarization state of light can be measured by passing the light through a phase retarder **W** followed by a linear polarizer (analyzer) **A** and measuring the transmitted intensity. For a beam of light

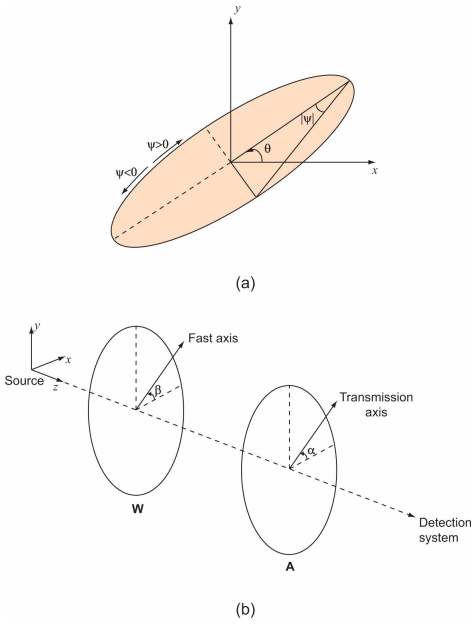

Figure 5.1: Determination of Stokes Parameters

with Stokes parameters (I, M, C, S) this transmitted intensity is determined by using Mueller calculus and is given by [**?**]

$$I_T(\alpha,\beta,\delta_r) = \frac{1}{2}[I + (\frac{M}{2}\cos 2\alpha + \frac{C}{2}\sin 2\alpha)(1+\cos\delta_r)] + \frac{S}{2}\sin\delta_r \sin(2\alpha - 2\beta)$$
$$+\frac{1}{4}[M\cos(2\alpha - C\sin 2\alpha)\cos 4\beta + (M\sin 2\alpha + C\cos 2\alpha)\sin 4\beta](1-\cos\delta_r) \tag{5.1}$$

where β and α are defined in Fig. 5.1 and δ_r is the phase shift caused by the retarder between electric field components along its fast and slow axes.

5.1 Stokes Parameters using Fourier Series Coefficients

In order to determine (I, M, C, S), the method is adopted from [**?**] which involves the measurement of the variation in transmitted intensity I_T as the retarder (β) is rotated for fixed α and δ_r. Since I_T is a sum of even sine and cosine harmonics, I_T measured as a function of β, forms a sum of Fourier components. In this experiment, the Fourier sine and cosine coefficients of the measured I_T versus β data are used to calculate the Stokes parameters from these coefficients by using the expressions

$$I = C_o - \frac{1+\cos\delta_r}{1-\cos\delta_r}[C_4\cos(4\alpha + 4\beta_o) + S_4\sin(4\alpha + 4\beta_o)] \tag{5.2}$$

$$M = \frac{2}{1-\cos\delta_r}[C_4\cos(2\alpha + 4\beta_o) + S_4\sin(2\alpha + 4\beta_o)] \tag{5.3}$$

$$C = \frac{2}{1-\cos\delta_r}[S_4\cos(2\alpha + 4\beta_o) - C_4\sin(2\alpha + 4\beta_o)] \tag{5.4}$$

$$S = \frac{-S_2}{\sin\delta_r\cos(2\alpha + 4\beta_o)} \tag{5.5}$$

Rotation angle θ is given by

$$\tan(2\theta) = \frac{C}{M} \tag{5.6}$$

Ellipticity angle ψ is given by

$$\sin(2\psi) = \frac{S}{I} \tag{5.7}$$

β_o is the initial angle between the fast axis and the x-axis and δ_r is the retardance of the QWP. C_o, C_2, C_4 are the cosine and S_2 and S_4 are the sine Fourier series coefficients of the intensity I_T. Subscripts represent the harmonic of the sine or cosine.

5.2 Experiment

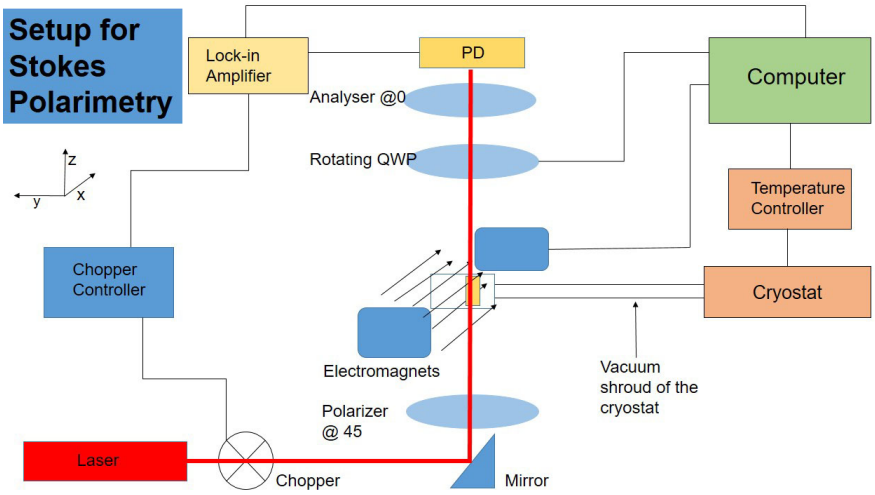

Figure 5.2: Stokes polarimetry schematic

[?] Figure 5.1 schematically illustrates the experimental setup. The light source was an intensity stabilized 633 nm Laser (Thorlabs,HNL100L). The transmission axis of the linear polarizer P was fixed at 45^o. The TGG crystal (Castech Inc.) was cylindrical in shape with a length of 1 cm and diameter of 3 mm. The laser beam was incident on the circular cross-section of the cylinder along the designated optical axis (z axis) of the uniaxial crystal. The crystal was mounted inside the vacuum shroud of the cryostat (Janis Research) using a devised clamping assembly made out of 99.9 percent pure copper. Thermal grease (Apiezon) was applied between the sample holder and the cold-head of the cryostat in order to maximize thermal conductivity. Fused quartz windows on the sides of the vacuum shroud allowed laser beam access to the crystal inside. A computer interfaced temperature controller (Model 331, LakeShore) was used to vary the temperature from 8100 K using a 25 W resistive heater while the temperature of crystal was monitored using a Gallium Arsenide diode temperature sensor (TG-120-CU-4L, LakeShore). An electromagnet (3470, GMW Associates) was used as the transverse magnetic field source. The electromagnets power supply (DLM60-10, Sorensen) as well as the temperature monitoring and control system were fully integrated using LABView allowing automated scanning of the magnetic field

and temperature for rapid measurements. The magnetic field B was controlled by varying the current passing through the electromagnet coils. The calibration constant relating current and magnetic field was pre-determined using a gauss meter (410-SCT, LakeShore).A 633 nm quarter wave plate (WPMQ05M-633, Thorlabs) was used as the retarder W which was mounted in a precision motorized rotation stage (PRM1/MZ8E, Thorlabs) allowing the angular displacement β to be varied with a resolution better than 0.1^o. The retardation δ_r at 633 nm was pre-determined as follows: I_T vs β was measured for light with known Stokes parameters, the Fourier coefficients for the data were determined and δ_r was calculated using Equation (9) [**?**]. The transmission axis of the analyzer A was fixed at $\alpha = 0$. The transmitted intensity I_T of the laser, after passing through all the aforementioned components, was measured by a photodetector configured in the photoconductive configuration. The photodetector was connected to the input of a lock-in amplifier (SR830, Stanford Research Systems) allowing phase sensitive detection. Lock-in amplifier is connected to the computer to store the readings from the lock-in amplifier. Optical chopper was used for modulation of light at 500 Hz and the reference signal for the lock-in amplifier is given from the optical chopper.

5.3 Results

Value of β_o was 3.6828^o and δ_r was found to be 86.2571^o

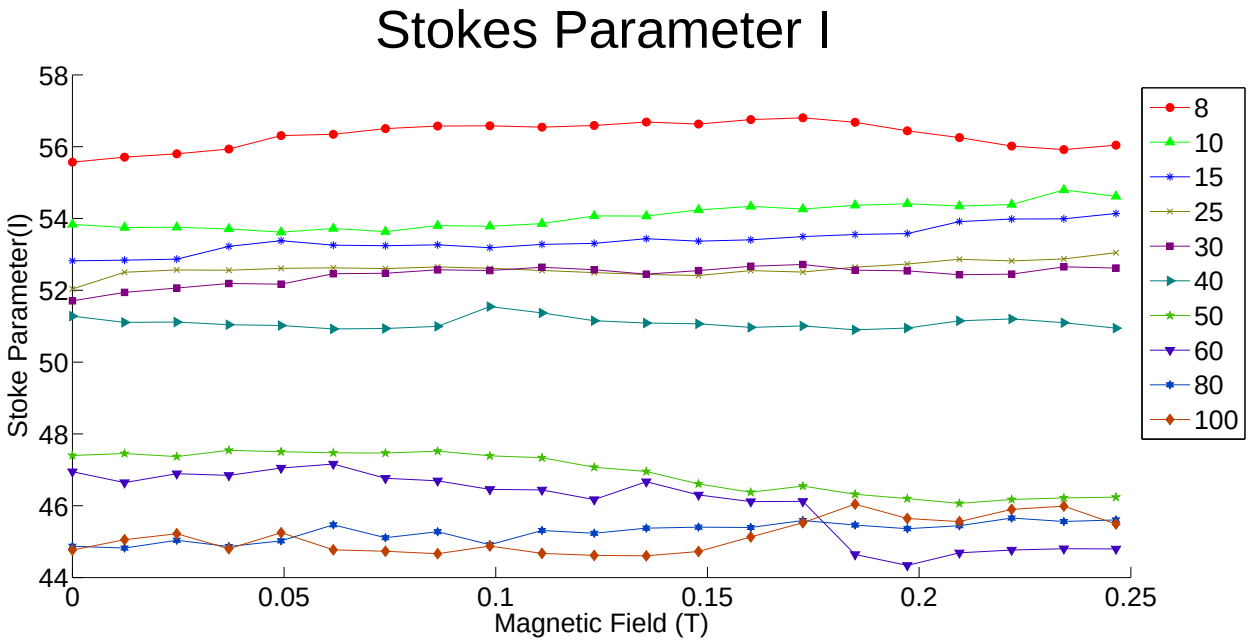

Figure 5.3: Parameter I (not normalized)

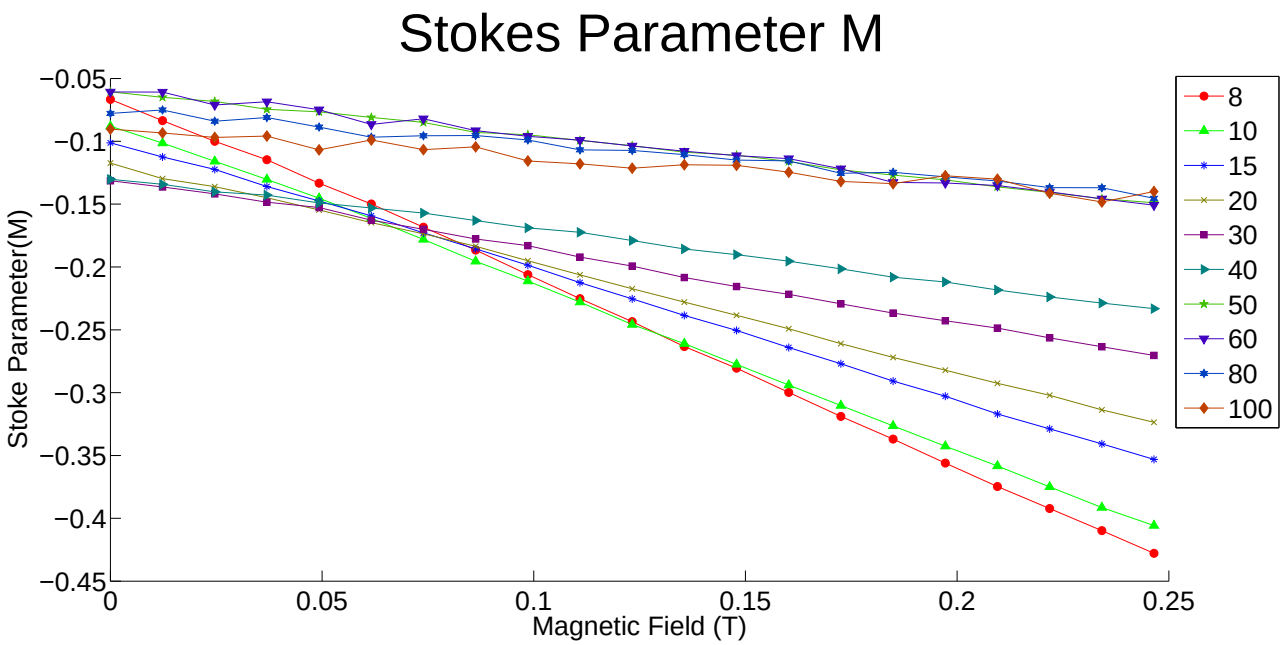

Figure 5.4: Parameter M

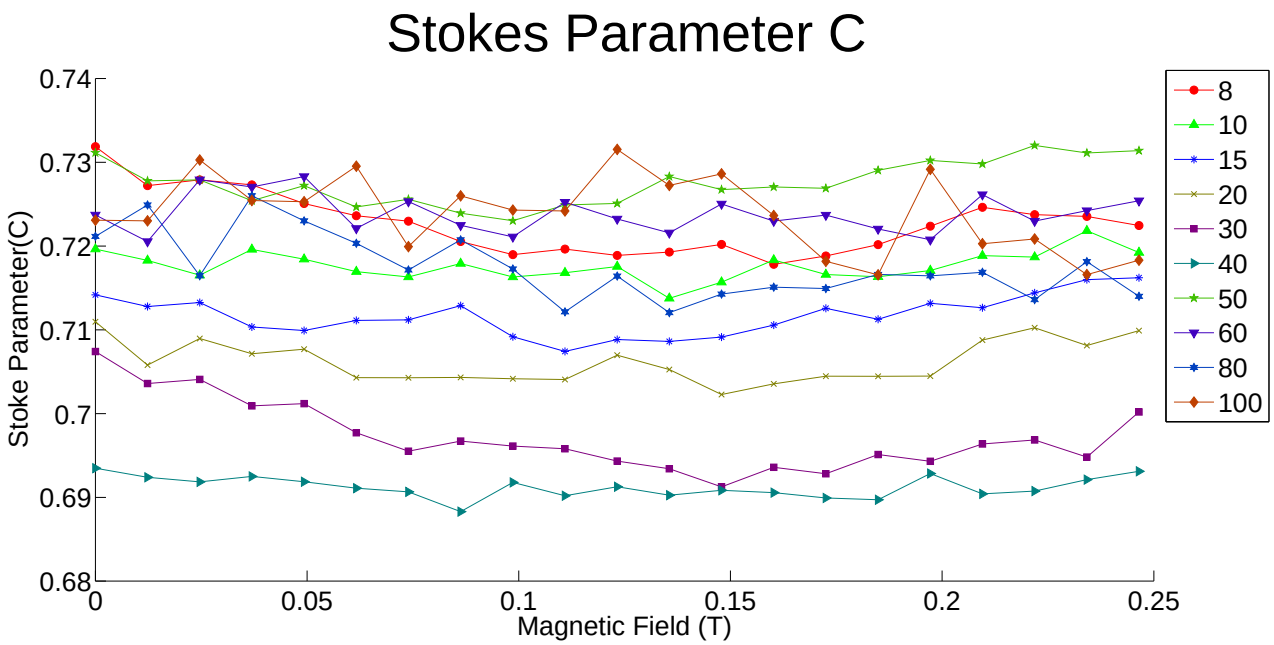

Figure 5.5: Paramter C

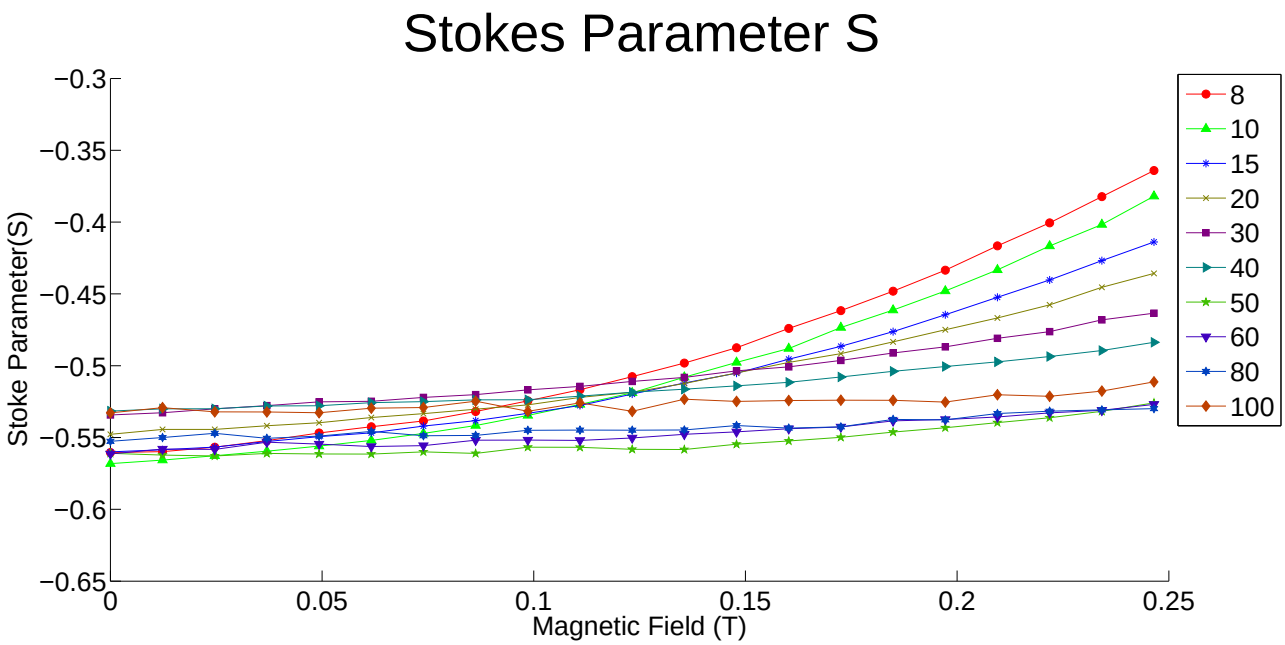

Figure 5.6: Parameter S

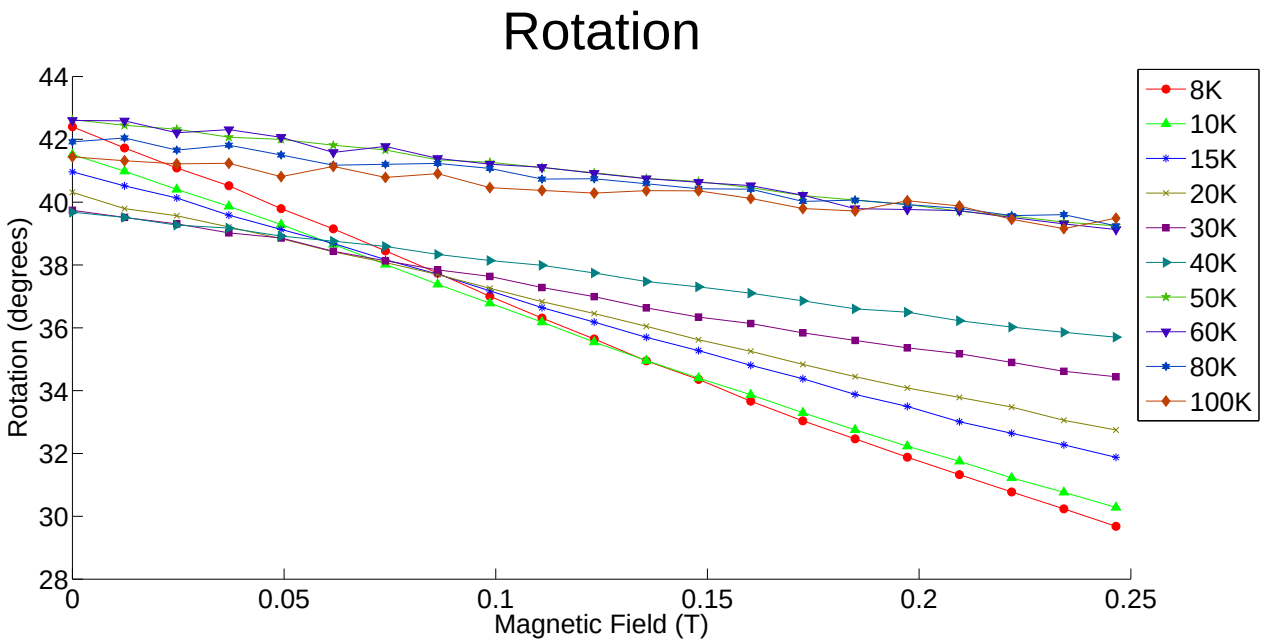

Figure 5.7: Rotation

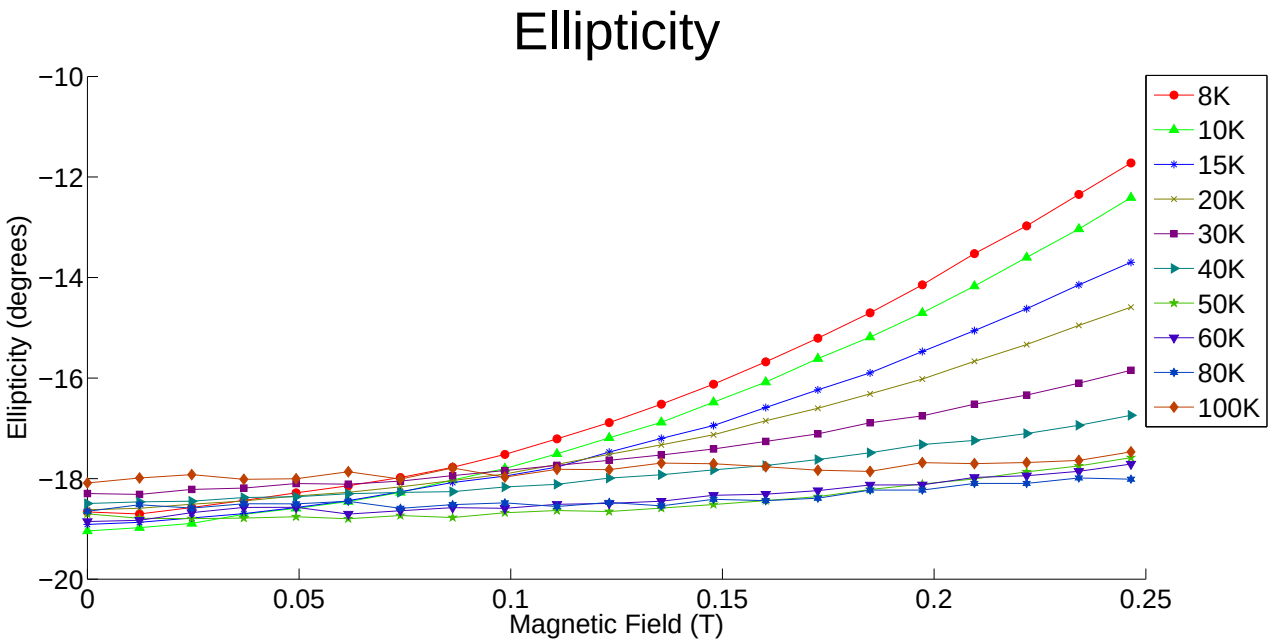

Figure 5.8: Ellipticity

Bibliography

[1] D. Clarke and J. F. Grainger. *Polarized Light and Optical Measurement*. Pergamon Press, 1971.

[2] Muhammad Sabieh Anwar, Hassaan Majeed, and Amrozia Shaheen. Analyzing combinations of circular birefringence, linear birefringence, and elliptical dichroism in magneto-optical rotators. *Journal of Modern Optics*, 62(1):75–84, 2015.

[3] V.A Kotov A.K Zvezdin. *Modern Magnetooptics and Magnetooptical Materials*. CRC Press, 1997.

[4] Aloke Jain, Jayant Kumar, Fumin Zhou, Lian Li, and Sukant Tripathy. A simple experiment for determining verdet constants using alternating current magnetic fields. *American Journal of Physics*, 67(8):714–717, 1999.

[5] Aysha Aftab Amrozia Shaheen and Muhammad Sabieh Anwar. Phase sensitve faraday rotation. *http://physlab.org/wp-content/uploads/2016/04/faraday2016$_v$5.pdf*, 2016.

[6] Amrozia Shaheen, Hassaan Majeed, and Muhammad Sabieh Anwar. Ultralarge magneto-optic rotations and rotary dispersion in terbium gallium garnet single crystal. *Appl. Opt.*, 54(17):5549–5554, Jun 2015.

[7] H. G. Berry, G. Gabrielse, and A. E. Livingston. Measurement of the stokes parameters of light. *Appl. Opt.*, 16(12):3200–3205, Dec 1977.

[8] Hassaan Majeed, Amrozia Shaheen, and Muhammad Sabieh Anwar. Complete stokes polarimetry of magneto-optical faraday effect in a terbium gallium garnet crystal at cryogenic temperatures. *Opt. Express*, 21(21):25148–25158, Oct 2013.